ICSV13 - Vienna
The Thirteenth International Congress on Sound and Vibration
Vienna, Austria, July 2-6, 2006

INVESTIGATION OF VIBRATION PHENOMENA IN LCD TRANSFER ROBOTS UNDERGOING LOW SPEED OPERATION

Hong Hee Yoo*[1], Phil Joo Cho[2], Ki Moon Lee[2], Hong Seok Lim[1] and Sung Hun Kwon[1]

[1]School of Mechanical Engineering, Hanyang University 17, Haengdang-Dong, Sungdong-Gu, Seoul 133-791, Korea

[2] SAMSUNG ELECTRONICS CO., LTD. 416, Maetan-3Dong, Yeongtong-Gu, Suwan-City, Gyeonggi-Do, 443-742, Korea

hhyoo@hanyang.ac.kr (e-mail address of the first author)

Abstract

During the operation of LCD transfer robots, excessive vibration phenomena often occur in low speed teaching mode. Even if the robot can be operated under normal speed without any vibration phenomena, the low speed teaching mode vibration still makes the robot operator feel uncomfortable and worried. To eliminate such low speed vibration from the robot, the cause of the phenomena should be identified. For the purpose, a multi-body model for the LCD transfer robot is developed in this study. It is shown that the numerical results obtained from the model are in reasonable agreements with experimental results. By employing the developed model, design parameters related to the low speed vibration are identified and an effective design guideline to reduce the low speed vibration in the LCD transfer robot is suggested.

INTRODUCTION

Recently, the size of LCD transfer robot increases continuously as the size of LCD panel increases. Consequently, excessive vibration problems frequently occur as the natural frequencies of the robot system decrease significantly (due to the significant increase of the robot mass). Therefore, many kinds of efforts have been made by several researchers to reduce several classes of vibration problems which occurred in LCD transfer robots.

Yen [1], Mimmi and Pennacchi [2], and Mohamed and Tokhi [3] investigated a method to reduce the robot vibration problems by modifying the route of driving motor speed. This technique is often called the input shaping (or the trajectory planning) technique and it is very effective to reduce the vibration. Lee[4] and Park[5] suggested another method to reduce the vibration problems by minimizing the reaction forces acting on the robot joints. Such minimization can be realized by constraining the route (or the motion) of the robot end effecter in a specific way. Kim, Jeong, Lee, and Lee [6] and Oh, Lee, and Kim [7] introduced a different method to reduce the robot vibration. In this method, by changing materials or structural topology, the mass of the robot is decreased while the stiffness and the damping of the robot are increased. Consequently, increased natural frequencies of the robot result in the reduction of the vibration problem. The main purpose of these methods mentioned so far is to reduce the vibration problems during the normal operation of the LCD transfer robot.

Different from the vibration problems occurred during normal operation, some vibration problems occur in a special operation mode of the LCD transfer robot. Some LCD transfer robots experience excessive vibration when they are operated under a low speed (this is often called the teaching mode). LCD transfer robots are usually operated in the teaching mode to check the safety of the route of the robot before normal operation. Even if no vibration problem occurs in normal operation, excessive vibration often occurs in a low speed teaching mode with the same robot. It can make the robot operator feel uncomfortable and worried. So such a vibration problem has to be resolved for comfortable operations of a LCD transfer robot.

The purpose of the present study is to identify the cause of the vibration problem occurred in LCD transfer robot operated in low speed and to establish a design guideline to eliminate such phenomena. For the purpose, a multi-body model for the LCD transfer robot by which dynamic characteristics of the robot can be estimated in a reliable way should be developed. By employing the model, the low speed vibration phenomena should be reproduced. Also design parameters related to the vibration phenomena will be identified and a design guideline for the robot to eliminate the vibration phenomena will be given.

MULTI-BODY DYNAMICS MODEL

Figure 1 shows the structure of the LCD transfer robot arm and the description of each part. In the present work, only the robot arm part is modelled because the main research interest is to control the vibration of the end point of the finger. Figure 2 shows a multi-body dynamics model which idealizes mechanical connection of the robot arm. Link motions are driven with belts and pulleys and the main power of the motion originates from a motor. Since the belts between the pulleys cannot be modeled with a multi-body dynamics element of a commercial code, it is idealized with forces and torques. Pulley and shaft are modeled as a single rigid body. The first shaft, the second shaft, and the third shaft are connected with spherical joints and the bushings. The first shaft and the first link, the second shaft and the second link, and the third shaft and the hand bracket are connected by pin joints. The reduction of the rotational motion (between two pulleys) is realized by coupler elements. Tensions of upper and lower belts are calculated first and then a torque and a resultant force acting on each pulley are calculated.

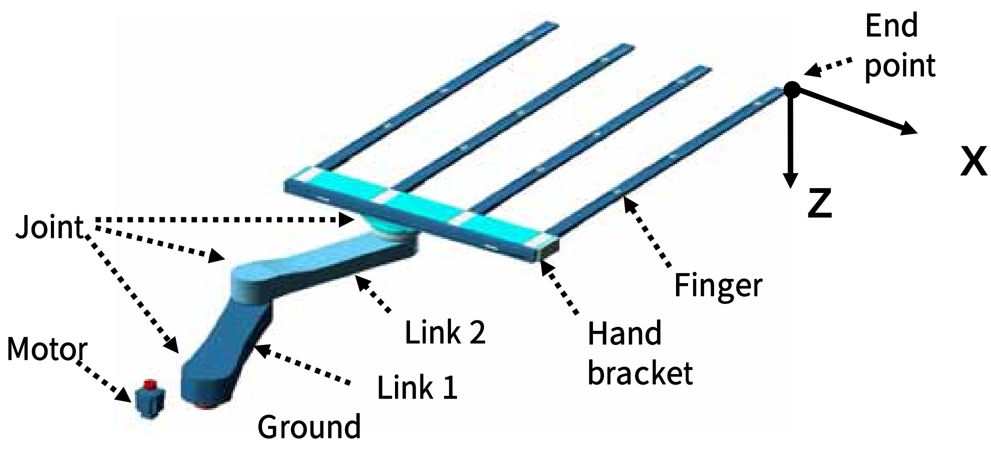

Figure 1. Configuration of the LCD transfer robot system

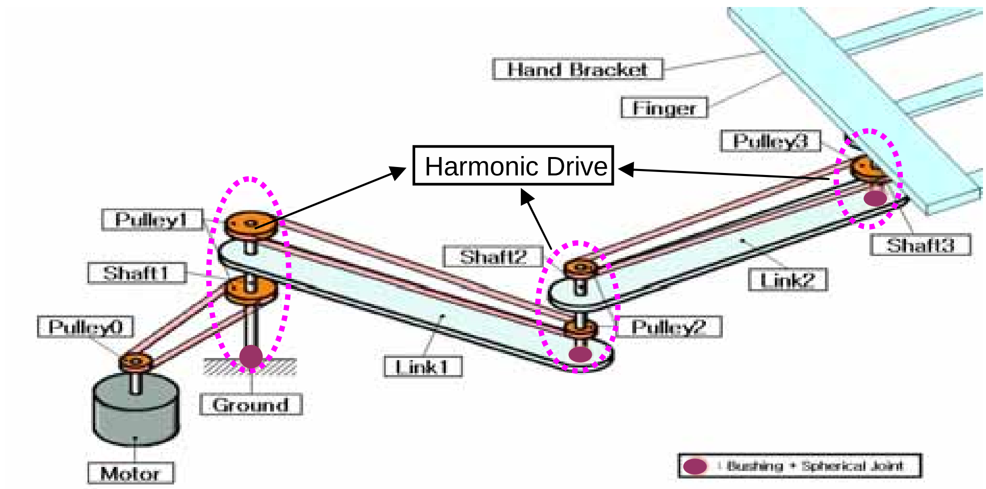

Figure 2 Multi-body dynamics modeling of the LCD transfer robot system

If the belt pretension is T_0, and the stiffness of belt is k, and the rotational angles of the two pulleys are θ_1 and θ_2, the upper and the lower belt tensions are calculated as

$$T_A = T_0 + k(r_1\theta_1 - r_2\theta_2)$$
$$T_B = \begin{cases} T_0 - k(r_1\theta_1 - r_2\theta_2), & \text{if} \quad T_0 - k(r_1\theta_1 - r_2\theta_2) > 0 \\ 0 \quad , & \text{if} \quad T_0 - k(r_1\theta_1 - r_2\theta_2) \le 0 \end{cases} \tag{1}$$

And the torques and the resultant forces acting on the two pulleys are calculated as

$$M_1 = -r_1(T_A - T_B), \qquad M_2 = r_2(T_A - T_B) \tag{2}$$

$$\vec{F}_1 = T_A(\cos\alpha\,\hat{i} + \sin\alpha\,\hat{j}) + T_B(\cos\alpha\,\hat{i} - \sin\alpha\,\hat{j})$$
$$\vec{F}_2 = -T_A(\cos\alpha\,\hat{i} + \sin\alpha\,\hat{j}) - T_B(\cos\alpha\,\hat{i} - \sin\alpha\,\hat{j}) \tag{3}$$

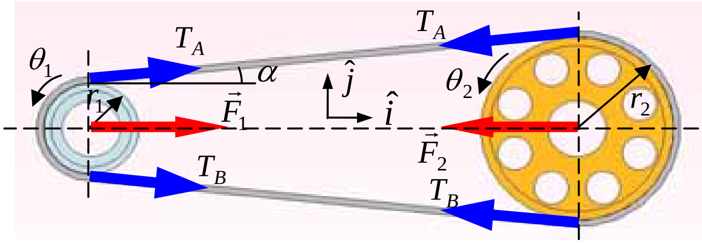

Figure 3 Dynamics model of belt-pulley system

Links and robot fingers have structural flexibilities. However, since their effects on the deflection of the end point are trivial, they are all modeled as rigid bodies. To measure the effects, the exciting frequency is compared with the structural natural frequency.

NUMERICAL RESULTS

In the modelling of the LCD transfer robot, mass eccentricities (which result from mass center dislocations of harmonic drives) are considered. These eccentricities are found to generate the excitation force to cause the low speed vibration. Important factors which determine the dynamic characteristics of the robot are the stiffness and the damping coefficients of the joint bushings. These factors are, however, hard to measure directly. So, the natural frequencies and the static deflection of the robot are measured experimentally to estimate the coefficients reversely. Table 1 shows the experimental and the numerical results of two natural frequencies and the static deflection of the robot in unfolded posture. Bending and torsional stiffness estimated from the results are also given in the table. As of damping constants, 0.2% of torsional stiffness is employed for the torsional damping and 0.02% of lateral bending stiffness is employed for the lateral damping. Torsional damping constant is higher than that of lateral damping since more friction occurs during the rotational motion of the robot links.

As the posture of the robot varies during the operation, the natural frequencies of the robot vary continuously. Figure 4 shows the lowest three natural frequencies and

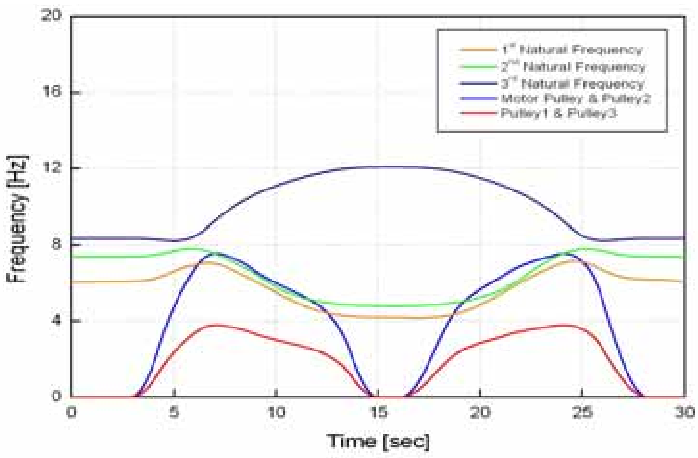

Figure 4 Rotating frequency of pulleys and natural frequency of robot (10% operating speed)

the rotating frequencies of pulleys in 10% operating speed. From these results, one can observe that the excitation frequency of the pulley 2 is close to the lowest two natural frequencies of the robot in some time interval. Therefore excessive vibration can occur.

By employing the developed multi-body modeling of the robot, transient analyses were performed for the low speed operation. Figure 5 and 6 show the vibration of the end point of the robot. The experimental results and the numerical results are shown in the figures. Even if the local shapes are not in exact agreement, the maximum peaks are similar. In Fig. 7, frequency response spectrums are compared. In the case of X-directional vibration, the two spectrums agree well in the 4-8Hz region. In the case of Z-direction, one can observe a vibration peak around 9.5Hz from the experimental result. Since the exciting frequency generated by the harmonic drive ranges from 4Hz to 8Hz in the low speed operation, the vibration peak around 9.5Hz should be caused by other reason, which could not be disclosed in the present work. Figure 8 shows the dynamic response of the robot in high speed operation. The maximum amplitude of the response is about 1mm during the operation but the amplitude becomes about 0.1mm at the LCD stacking stage (around 4 sec). Thus, this robot can be employed for the normal stacking operation without any trouble.

METHOD OF VIBRATION REDUCTION IN LOW SPEED OPERATION

In this section, a design guideline to reduce the vibration in low speed operation is proposed for the LCD transfer robot. For the purpose, the torsional stiffness is chosen as a design parameter since it (which is equivalent to the torsional stiffness of the harmonic drive) can be effectively controlled. However, the bending stiffness is not chosen as a design parameter since it depends on the boundary condition where a harmonic drive and two links are connected. The boundary condition is not practically controllable. Figure 9 shows the variation of the maximum amplitude of the vibration as the torsional stiffness of each joint varies. One can observe that the size of maximum amplitude decreases as the torsional stiffness of the first joint increases. On the other hands, as the torsional stiffness of the second and the third joints decrease, the maximum amplitude decreases. Figure 10 shows the effects of mass center positions of the hand bracket and the finger on the maximum vibration amplitude. The results indicate that the maximum vibration amplitude decreases as the mass center of hand bracket and the finger moves to the positive direction.

Table 1 Joint stiffness, natural frequency and static deflection of the robot
(※( ) – experimental data)

Joint	Joint1 [N-mm/deg]		Joint2 [N-mm/deg]		Joint3 [N-mm/deg]		Natural frequency [Hz]	Static deflection [mm]
Joint stiffness	Bending	12.52E6	Bending	5.51E6	Bending	1.81E6	4.80(4.38)	26.3(22.0)
	Torsion	6.28E6	Torsion	5.65E6	Torsion	4.54E6	4.12(4.38)	

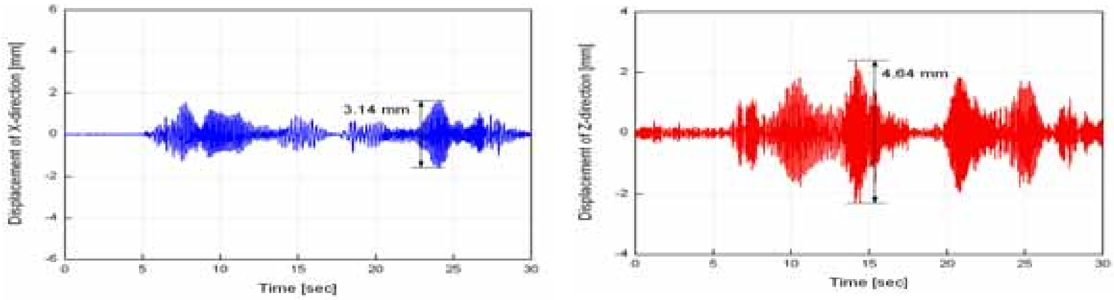

(a) X-direction *(b) Z-direction*

Figure 5 Dynamic response of the robot obtained by experiment (10% operating speed)

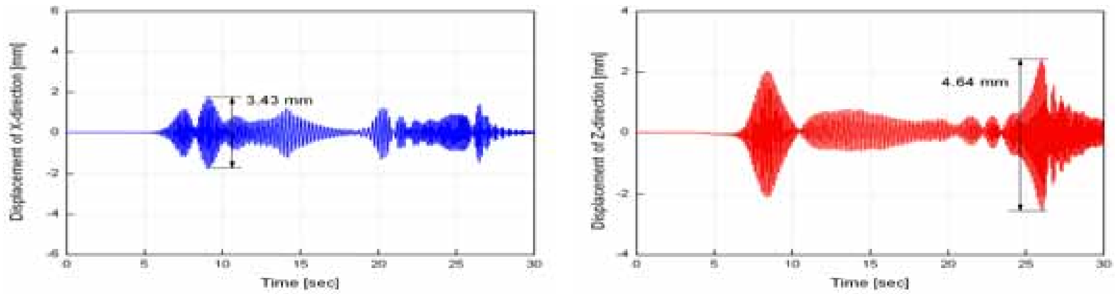

(a) X-direction *(b) Z-direction*

Figure 6 Dynamic response of the robot obtained by simulation (10% operating speed)

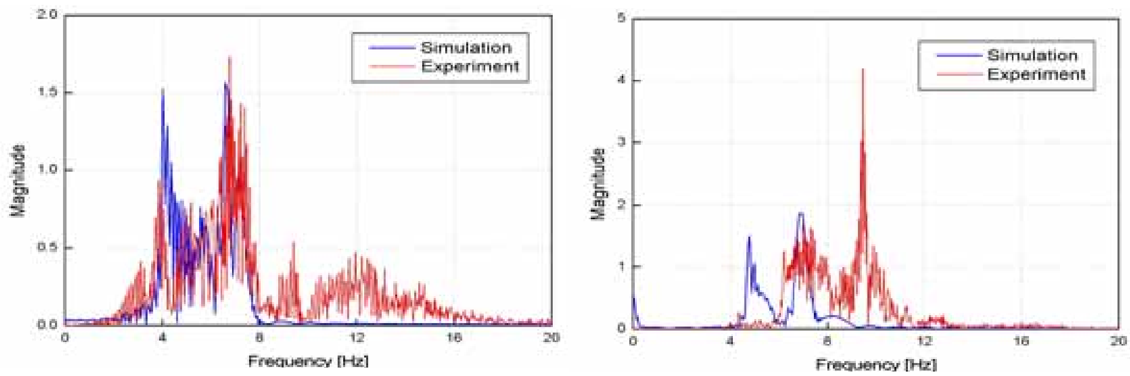

(a) X-direction *(b) Z-direction*

Figure 7 Comparison of frequency response spectrum of the robot (10% operating speed)

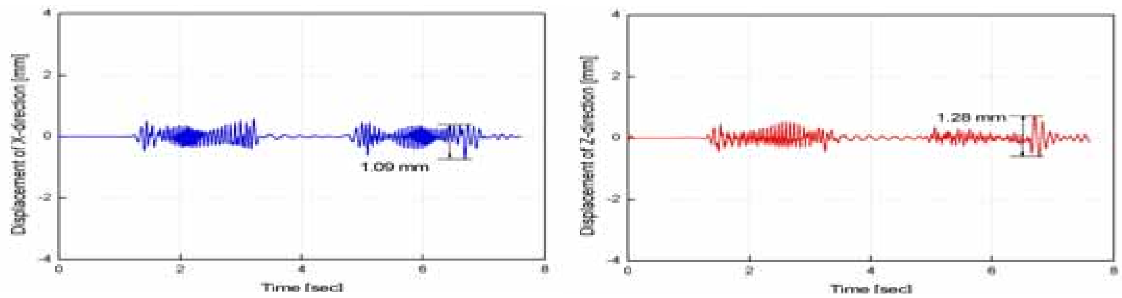

(a) X-direction *(b) Z-direction*

Figure 8 Dynamic response of the robot obtained by simulation (100% operating speed)

The LCD transfer robot design procedure to avoid excessive vibration in low speed operation can be summarized as follows:

(1) By employing multi-body dynamics model, the modal and transient analyses are performed to see if excessive vibration occurs in low speed operation.

(2) By comparing excitation frequencies of harmonic drives with the natural frequencies of the robot, possibility of resonance needs to be checked.

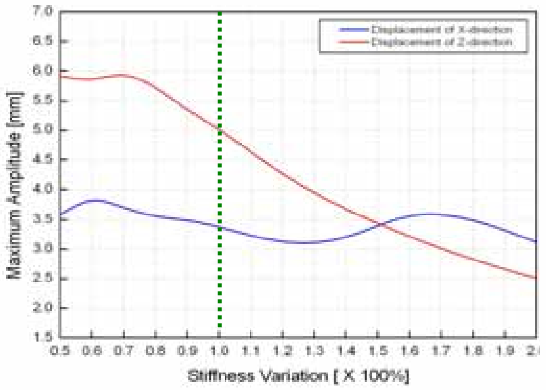

(a) Torsional stiffness of 1st joint

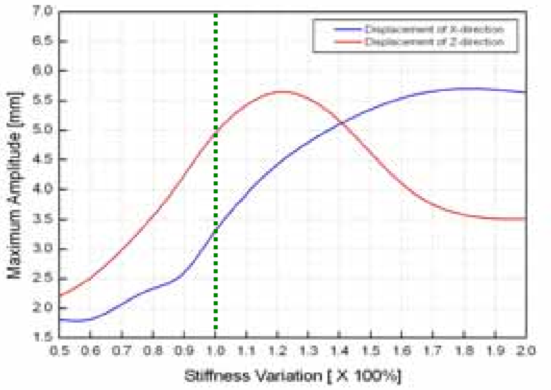

(b) Torsional stiffness of 2nd joint

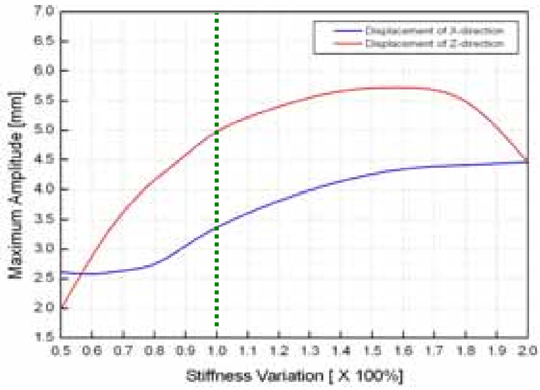

(c) Torsional stiffness of 3rd joint

Figure 9 Variation of maximum amplitude versus torsional stiffness of joint

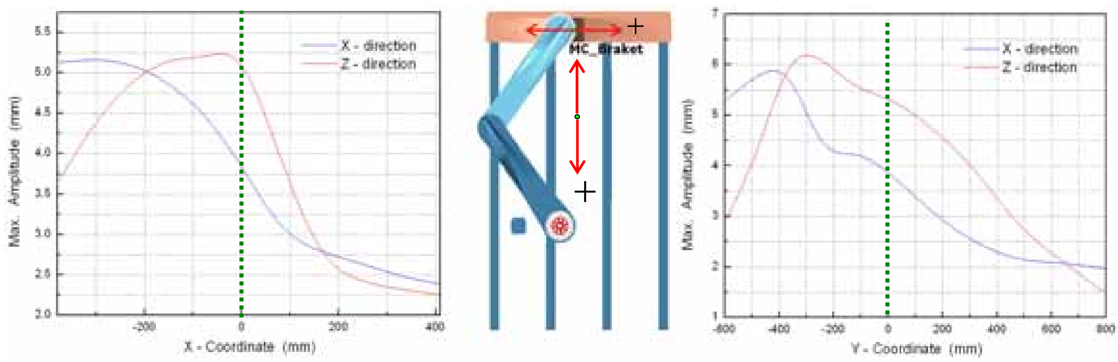

(a) Hand bracket *(b) Finger*

Figure 10 Variation of maximum amplitude versus mass center position of robot

(3) If the vibration amplitude is small, the design is acceptable. However, if the vibration amplitude exceeds a certain value, new design parameters for the LCD transfer robot need to be found.
(4) Torsional stiffnesses of harmonic drives are the first group of design parameters. By modifying the stiffnesses, the vibration amplitude can be reduced effectively.
(5) Mass center positions of the hand bracket and the finger are the second group of design parameters. By changing the positions, additional vibration reduction can be achieved.

CONCLUSION

In this paper, the major cause of excessive vibration occurring in low speed operation of LCD transfer robot is investigated. For the investigation, a multi-body modeling of the robot is developed and the modal and the transient analyses are executed. The torsional and the bending stiffness of the joints of the robot can be estimated by employing the experimental results of natural frequencies and the static deflection of the robot. The possibility of excessive vibration can be first identified by comparing the rotating frequencies of harmonic drives and a few lowest natural frequencies of the robot. Then with the transient analysis results, the vibration amplitude can be found. To reduce the vibration amplitude in low speed operation, design parameters such as the torsional stiffness of harmonic drives and mass center location of hand bracket and finger can be modified.

ACKNOWLEGMENTS

This research was supported by SAMSUNG Electronics Co. for which the authors are grateful.

REFERENCES

Periodicals: G. G. Yen, “Distributive vibration control in flexible multibody dynamics”, Computer and Structures, **Vol. 61, No. 5**, pp. 957-965 (1996).

Periodicals: G. Mimmi and P. Pennacchi, “Pre-shaping motion input for a rotating flexible link”, International Journal of Solids and Structures, **Vol. 38,** pp. 2009-2023 (2001).

Periodicals: Z. Mohamed and M. O. Tokhi, “Command shaping techniques for vibration control of a flexible robot manipulator”, Mechatronics, **Vol. 14,** pp. 69–90 (2004).

Periodicals: H. P. Lee, “Motions with minimal base reactions for redundant manipulators”, Computer and Structures, **Vol. 61, No. 4,** pp. 651-656 (1996).

Periodicals: K. J. Park, “Flexible robot manipulator path design to reduce the endpoint residual vibration under torque constraints”, Journal of Sound and Vibration, **Vol. 275**, pp. 1051–1068 (2004).

Periodicals: Y. G. Kim, K. S. Jeong, D. G. Lee and J. W. Lee, “Development of the composite third robot arm of the six-axis articulated robot manipulator”, Composite Structure, **Vol. 35,** pp. 331-342 (1996).

Periodicals: J. H. Oh, D. G. Lee and H. S. Kim, “Composite robot end effecter for manipulating large LCD glass panels”, Composite Structure, **Vol. 47**, pp. 497-506 (1999).

Books: MSC Software INC, MSC.ADAMS 2003 User’s manual (2003).